UCID- 18784

Confinement of Alpha Particles In Tandem Mirrors

R. S. Devoto
M. Ohnishi*

September 8, 1980

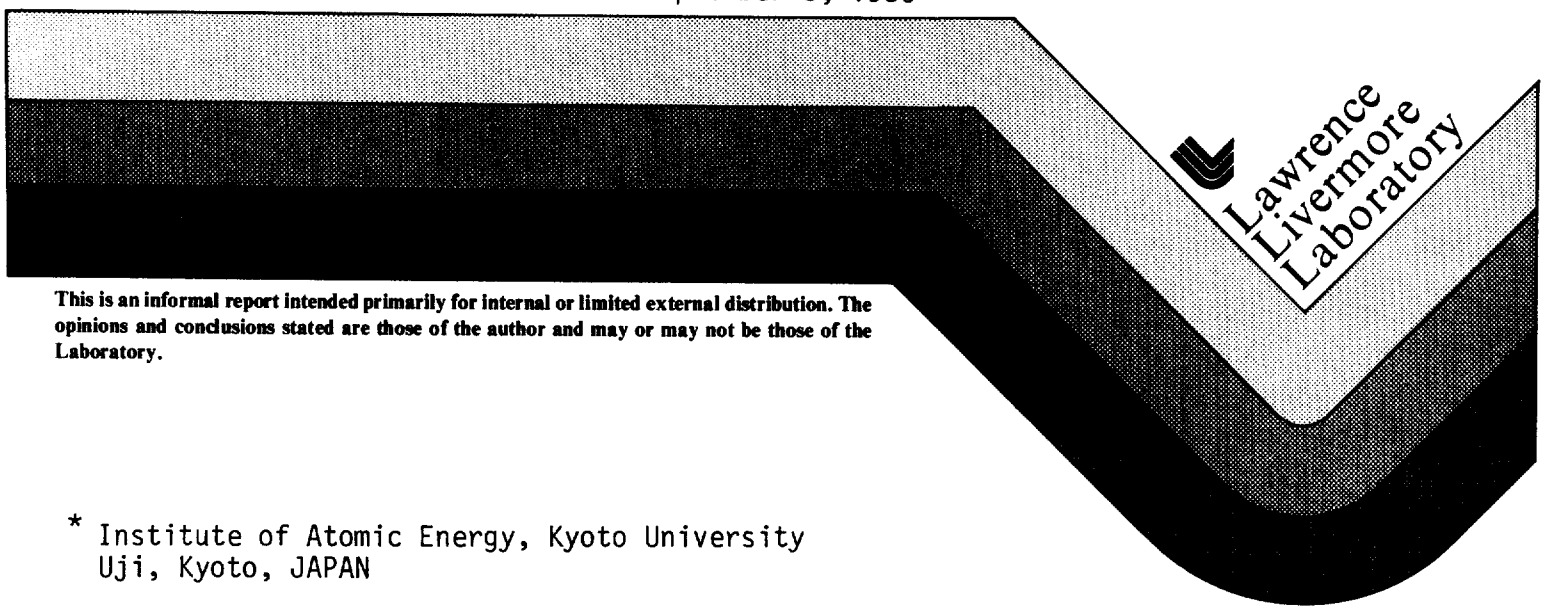

* Institute of Atomic Energy, Kyoto University
Uji, Kyoto, JAPAN

CONFINEMENT OF ALPHA PARTICLES IN TANDEM MIRRORS*

R. Stephen Devoto, Masami Ohnishi**

Lawrence Livermore National Laboratory, University of California

Livermore, California 94550

ABSTRACT

Mechanisms leading to loss of alpha particles from non-axisymmetric tandem mirrors are considered. Stochastic diffusion due to bounce-drift resonances can cause rapid radial loss of high energy particles but can be suppressed by imposing a 20% rise in axisymmetric field before the quadrupole transition sections. With this field, radial losses due to resonances should be minimal until alpha particles near thermal energies, when they enter the resonance plateau regime. Retention in the plasma of 60-80% of alpha-particle energy appears possible; precise calculation requires computation of drift orbits, of which two typical examples, resonant and non-resonant, are presented.

*Work performed under the auspices of the U.S. Department of Energy by the Lawrence Livermore National Laboratory under contract number W-7405-ENG-48.

**Institute of Atomic Energy, Kyoto University, Uji, Kyoto, JAPAN

I. Introduction

In studies of tandem mirror reactors, it is generally assumed that the bulk of alpha-particle kinetic energy is transferred to the fuel ions and electrons, the alpha particles being lost when they reach thermal energies. Since they are initially only magnetically confined, a fraction is born in the loss cone and lost in a transit time. This fraction is

$$f \approx 1/2\ R$$

where R is the ratio of the maximum B field to the true field in the central cell. The maximum field will generally be the plug mirror field but could be the outer field in an outer thermal barrier configuration. For typical conditions $f \approx$ 10-15%.

When the alpha-particle energy $\epsilon \leq Z_i\phi_i$, where ϕ_i is the center cell confining potential, then potential confinement is important and axial confinement time follows the Pastukhov relation

$$n\tau_c \sim n\tau_{ii}\ (Z_i\phi_i/T_i)\ \exp\ (Z_i\phi_i/T_i)$$

where τ_{ii} is the ion-ion collision time and Z_i and T_i are the ion charge and temperature. We see that thermal alpha-particles are confined better than fuel ions by the factor 2 exp $(\phi_i/T_i) \approx 25$. Thus, to prevent ash build-up, alpha particles must be lost radially, either as they drag down in energy or after thermalization.

Mechanisms for radial losses in non-axisymmetric tandem mirrors have been identified by Ryutov and Stupakov.[1] The major mechanism involves particles which drift azimuthally by odd multiples of $\pi/2$ as they pass from one mirror to the other, the so-called resonant particles.

The locations of the resonances depend on the plasma model adopted and, most importantly, on the velocity pitch angle $\theta = \sin^{-1}(V_\perp/V)$. In the next section, the resonance locations in phase space for alpha particles are obtained with the aid of a model suitable for reactors.

Three types of diffusion are associated with the presence of resonances: resonant banana, in which ions have adequate time to trace out bananas before collisions, resonant plateau, where banana orbits are interrupted by collisions before completion, and stochastic diffusion, which arises when resonant ions suffer large enough radial deflection on each reflection to move them to another resonance surface. Some consideration of the applicability of these different mechanisms to alpha-particle transport is given in the second section.

These initial considerations show that it is necessary to compute alpha-particle trajectories. As a first step, we describe a program which fits a long-thin approximation to the magnetic fields to the output from the EFFI code.[2] In the last section some typical orbits, including resonant orbits, are described.

II. Alpha-Particle Resonances

The conditions for resonance are

$$|\Delta\psi| = k\pi/2 \qquad k = 1,3,5,..... \tag{1}$$

where $\Delta\psi$ is the amount of azimuthal drift between reflections. The condition $k = 0$ in Eq. (1) corresponds to non-resonant banana orbits.[1] Although a certain amount of azimuthal drift occurs due to field line curvature in the transition region, the dominant amount for $|\Delta\psi| >> 0$ is due to $\underset{\sim}{E} \times \underset{\sim}{B}$ and grad $|\underset{\sim}{B}|$ in the central cell of length L_c. We find

$$\Delta\psi = \frac{L_c}{r v_{\parallel} B}\left(\frac{d\phi}{dr} + \frac{\epsilon \sin^2\theta}{zeB}\frac{dB}{dr}\right) \tag{2}$$

In order to proceed further, we must adopt a plasma model. We assume uniform electron and ion temperatures and utilize the long thin approximation relating vacuum fields, B_v, to true fields. It has been argued by Ryutov and Stupakov[1] that the rapid radial mixing of electrons in the plugs will ensure uniform T_e. The temperature of the fuel ions would be expected to vary with radius, although initial computations for TMX show little variation.[3] For the density profile

$$n = n_0 f(x), \qquad x \equiv r/r_p \tag{3}$$

we find

$$\phi = T_e \ln f + \text{constant} \tag{4}$$

and

$$B^2 = B_v^2 (1 - \beta_0 f) \tag{5}$$

where β_0 is the plasma β at r=o. Equation (2) becomes

$$\Delta\psi = \frac{\sqrt{2m}\, L_c \quad (f' / r\, r_p f)}{2\epsilon^{1/2} \cos\theta \; B_v \, (1-\beta_0 f)^{1/2}} \cdot$$

$$\left[T_e - \frac{\epsilon \sin^2 \theta \; \beta_0 f}{2 Z \; (1 - \beta_0 f)}\right] . \tag{6}$$

m is the alpha-particle mass, ϵ its energy and Ze its charge.

It is evident from Eq. (6) that the dependence of $\Delta\psi$ on r is strongly dependent on the form of f. For a power-like law

$$f = (1 - x^{\gamma})^{\delta}, \; \gamma, \; \delta > 1 \tag{7}$$

$\Delta\psi \to \infty$ as $r \to r_p$, a clearly undesirable trait. Another, more desirable function involves an exponential,

$$f = \exp(-x^{\gamma}) \tag{8}$$

For the Gaussian form ($\gamma = 2$), f'/rf is a constant and $\Delta\psi$ has only weak dependence on r in the core of the plasma. Thus, $\Delta\psi$ will vary little as an ion is deflected radially at each mirror and the particle will tend to migrate radially out of the machine if it is on a resonance. A certain amount of control over the radial profile is available via choice of beam aiming, etc., and it is likely that the profile in a reactor will be flatter in the center than a Gaussian profile. We choose $\gamma = 4$ for the balance of this work, yielding

$$\Delta\psi = -\frac{2.89 \times 10^{-4} M^{1/2} L_c x^2}{\epsilon^{1/2} \cos\theta \; r_p^2 \; B_v (1 - \beta_o f)^{1/2}} \cdot \left[T_e - \frac{\epsilon \sin^2\theta \; \beta_o f}{2Z(1 - \beta_o f)}\right] \tag{9}$$

for T_e and ϵ in eV, M the alpha-particle mass in units of proton mass, and other quantities in the SI.

At low ϵ or vanishing β_o the form of the resonant curves is quite simple: lines of constant $V_{\parallel} = V \cos\theta$. Neglecting the second term of Eq. (9), the low-β limit for the k resonance is

$$\epsilon_{\parallel}(\beta = 0) = \frac{3.4 \times 10^{-8} M (L_c T_e)^2 x^4}{k^2 r_p^4 B_v^2 (1 - \beta_0 f)} \tag{10}$$

As $V_{\parallel} \rightarrow 0$ the number of resonance increases without bound, except for the value of $V_{\perp} = V \sin \theta$ where the quantity in brackets in Eq. (9) vanishes. The latter condition yields (non-resonant) bananas[1] and marks the division between β-dominated resonances occuring at higher $V_{\perp}$ and $\underset{\sim}{ExB}$ dominated resonances occurring at lower $V_{\perp}$. The energy separating these two regions is

$$\epsilon_{\perp}(k=0) = 2 Z T_e (1/\beta_o f - 1) \qquad (11)$$

and varies from a few times T_e at small r to very large energies at large r ($f \rightarrow o$). Thus, all resonances at large radii are governed by $\underset{\sim}{ExB}$ drift.

To show the explicit form of the resonant curves for alpha particles, we can consider a particular device, the Tandem Mirror Next Step (TMNS), currently under study. Representative parameters for this machine are given in Table I. Resonant curves are given in Figs. 1-4 at plasma radii of 10(f = .999), 20 (f = .98) 40(f = .74) and 60 cm (f = .22). Near the axis, (Fig. 1) the resonant curves are confined to small values of θ while at moderate radii (Figs. 2-3) resonances extend nearly to the loss cone. Thus, near the reactor axis, where the alpha-particle production rate is highest, it is unlikely that alpha-particles will be lost radially before reaching thermal energies. Whether or not the thermalized alpha particles will accumulate to densities sufficient to "poison" the reaction can be answered definitively only by diffusion computations[3] which include both fuel and alpha ions.

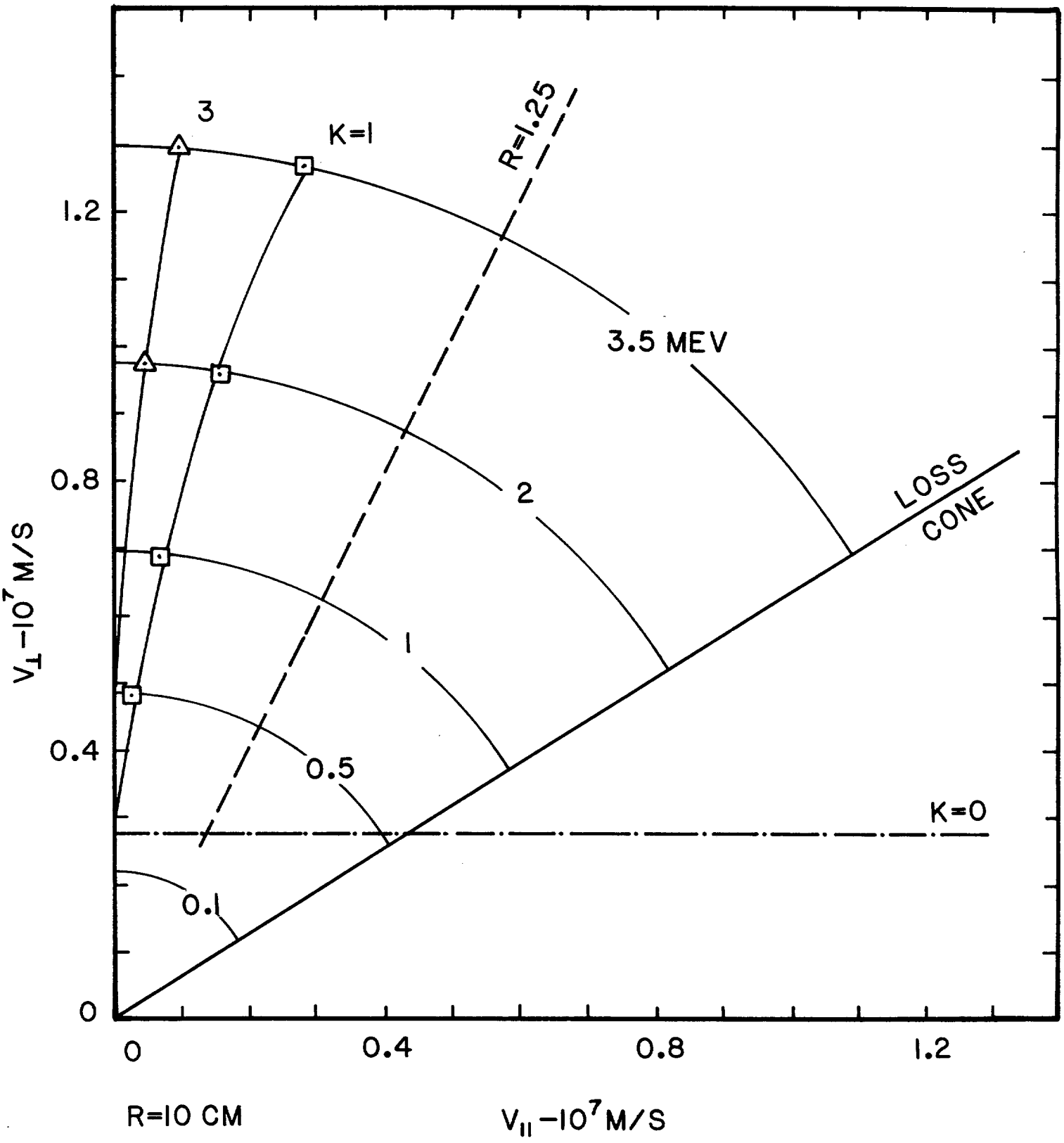

Fig. 1 Resonance curves for TMNS at r = 10 cm. Modification of loss-cone due to electrostatic potential not shown.

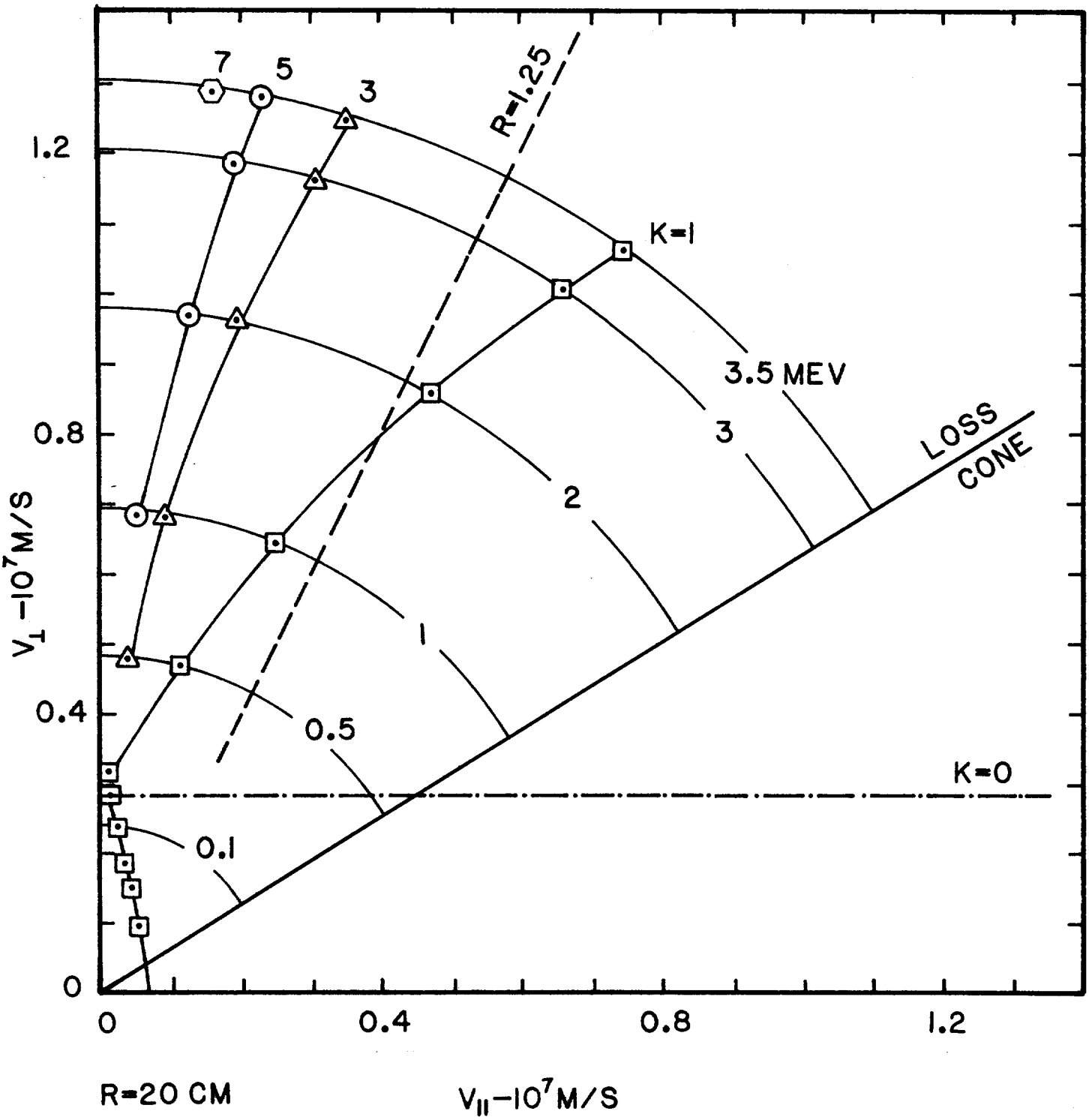

Fig. 2 Resonance curves for TMNS at r = 20 cm. Modification of loss-cone due to electrostatic potential not shown.

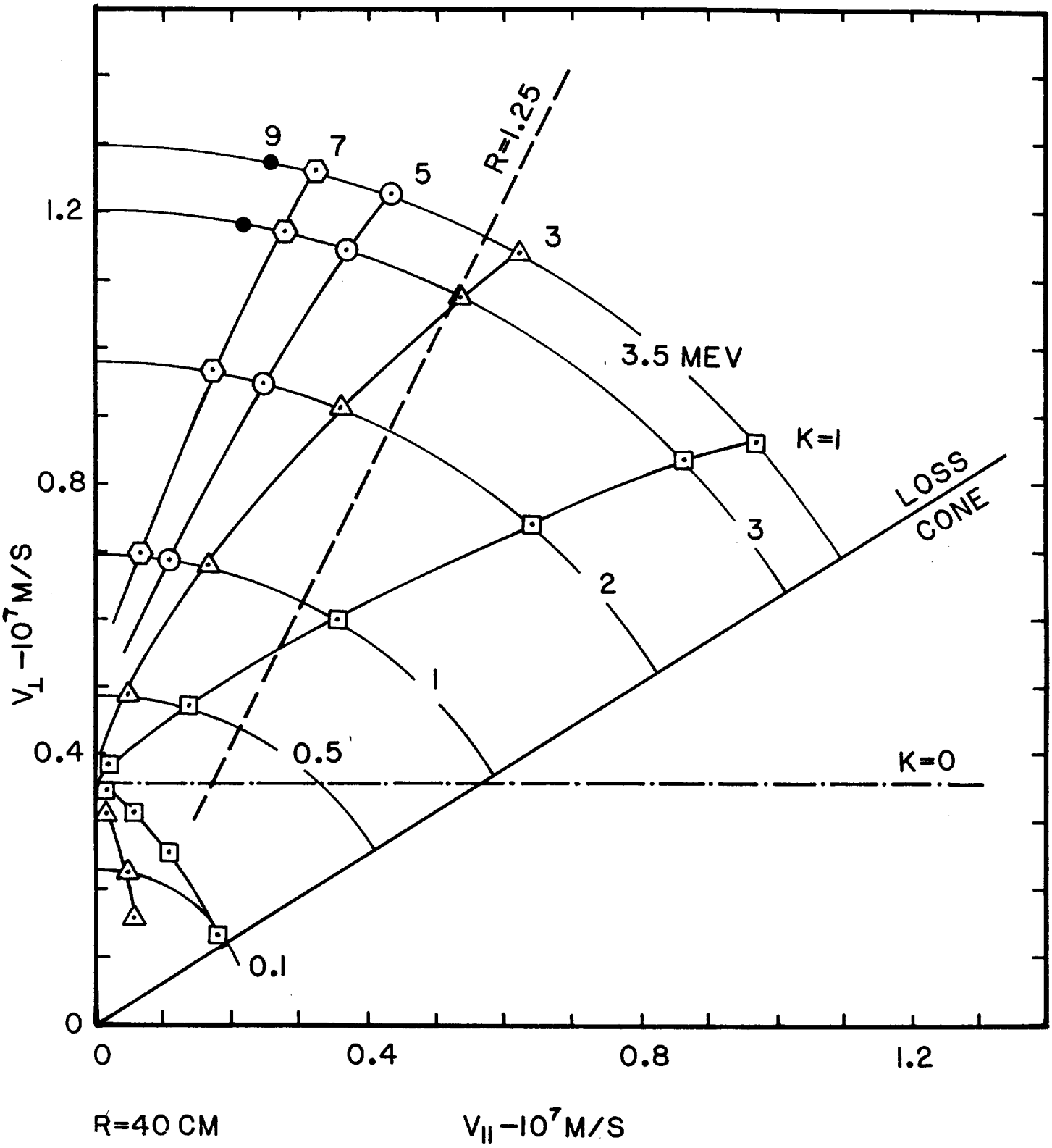

Fig. 3 Resonance curves for TMNS at r = 40 cm. Modification of loss-cone due to electrostatic potential not shown.

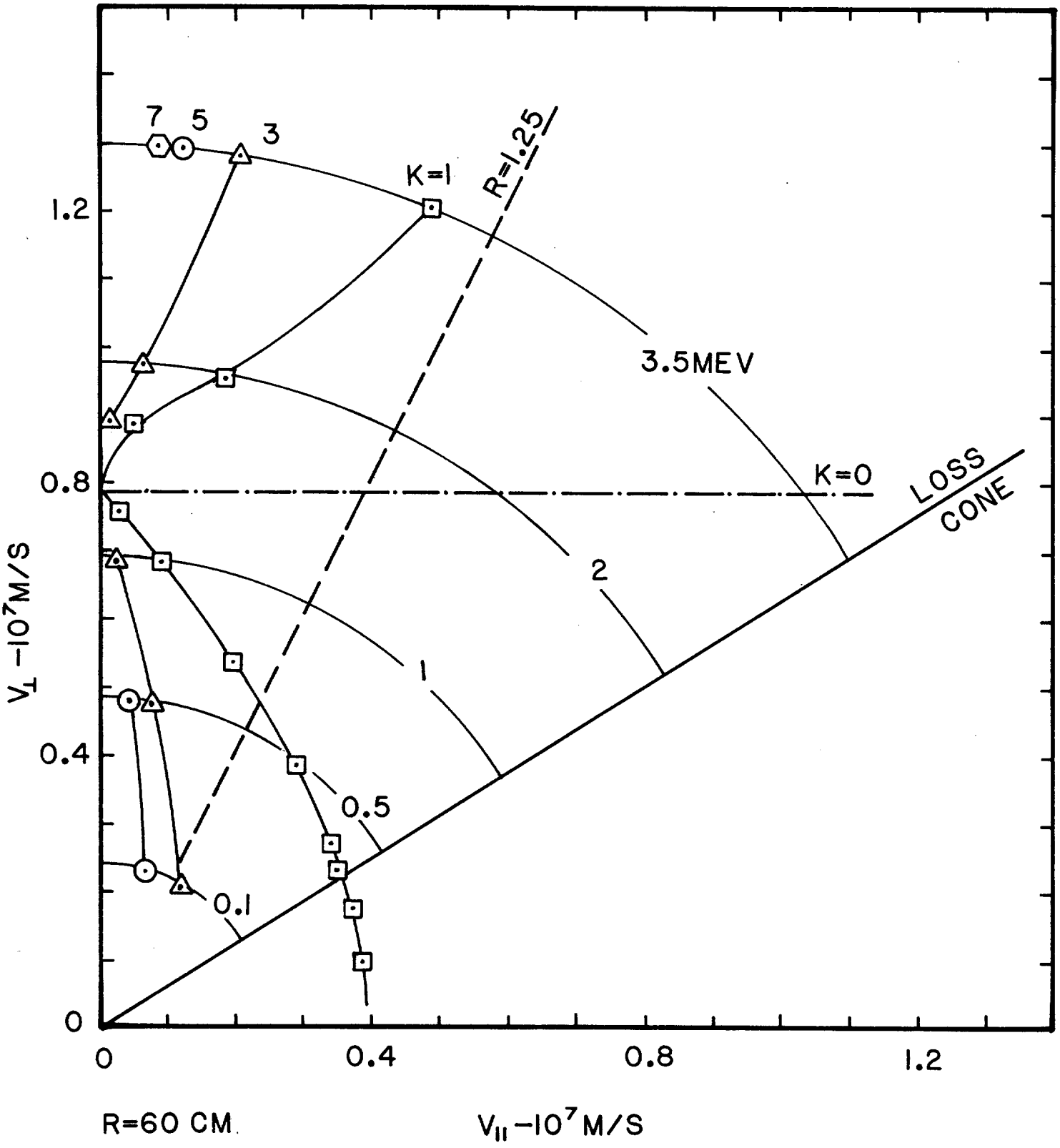

Fig. 4 Resonance curves for TMNS at r = 60 cm. Modification of loss-cone due to electrostatic potential not shown.

The large number of resonances at moderate radii (Fig. 3) seem to indicate that radial losses could be substantial. However, the radial deflection on many of these resonances can be eliminated by a modest axisymmetric mirror before the quadrupole field rise.[4] The boundary for a mirror ratio of 1.25 is shown in Figs. 1-4. Essentially, all resonances with $k > 1$ are removed, i.e., have $\delta r = 0$ for $r = 20$, 40 cm and none remain for $r = 10$, 60 cm. The mirror ratio corresponds to a lower vacuum mirror ratio when the axially uniform plasma pressure is taken into account. We find

$$R_v = R \left[1 - \beta_0 (1 - 1/R) \right]^{1/2} \tag{12}$$

and $R_v = 1.19$ for $R = 1.25$ at $\beta_0 = 0.5$.

The imposition of an axisymmetric mirror could have a disadvantageous effect on thermalized alpha particles by removing the mechanism for their removal. We can examine this question with the aid of Fig. 5 which shows the low energy region of Fig. 3 for $r = 40$ cm. We see that alpha-particles having energy below 150 keV will still experience resonant diffusion. An equivalent plot for $r = 10$ cm shows the resonant region only at much lower energies.

It should be emphasized that the results of this section are strongly dependent on L_c. Larger values of L_c will cause all resonant curves to shift to higher values of $V_{\parallel}$, thus moving more resonances into the region where quadrupole effects are important. The transition between β-dominated and $\underset{\sim}{E} \times \underset{\sim}{B}$ dominated resonances depends only on T_e, β_0 and the assumed profile and will remain fixed in phase space.

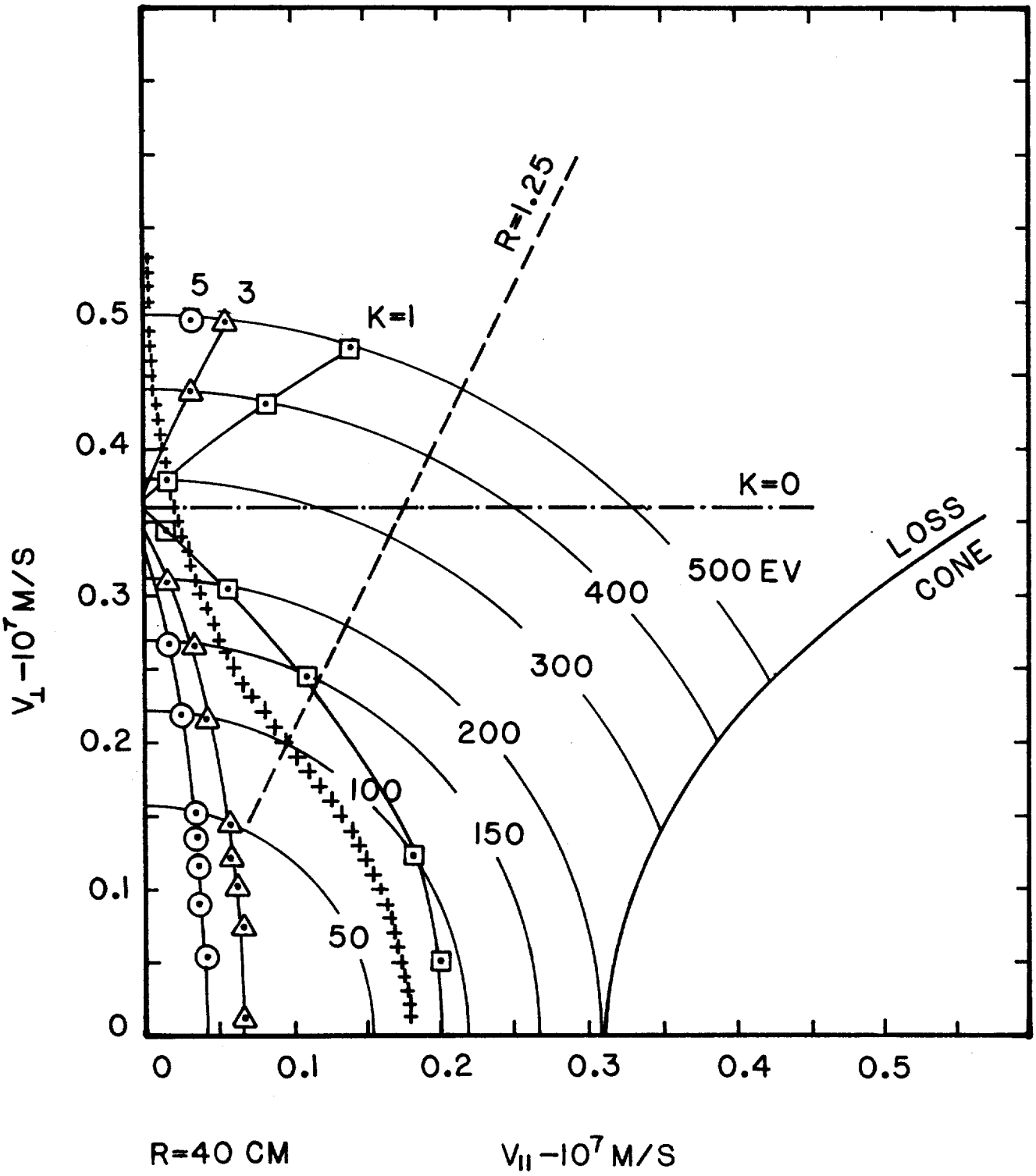

Fig. 5 Low-energy portion of Fig. 5 with schematic of loss-cone due to electrostatic potential = 100 keV indicated. +++: approximate boundary between resonant banana and resonant plateau diffusion [see Eq. (19).]

III. Diffusion

Ryutov and Stupakov[1] suggest that high energy alpha particles would be in the stochastic regime where the diffusion coefficient is independent of collision frequency

$$D \sim (\delta r)^2 \epsilon^{1/2} \cos\theta / L_c \tag{13}$$

The condition for stochastic diffusion is

$$\xi = \left|\frac{\delta r}{r}\right| r \left|\frac{\partial \Delta\psi}{r}\right| > 1 \tag{14}$$

at a resonance. We can evaluate this expression from Eq. (9),

$$\xi = \left|\frac{\delta r}{r}\right| \frac{5.8 \times 10^{-4} M^{1/2} L_c x^2}{\epsilon^{1/2} \cos\theta\, r_p^2 B_v \sqrt{g}} \cdot$$

$$\left[\left(\frac{x^4 \beta_0 f}{g} - 1 \right) T_e - \left(\frac{3 x^4 \beta_0 f}{g} - 1 \right) \frac{\epsilon \sin^2\theta \, \beta_0 f}{2 Z g} \right] \tag{15}$$

with $g \equiv 1 - \beta_0 f$.

In order to evaluate the criterion of Ineq. (14), we obtained values for $(\delta r/r)$ using a code[5] which computes guiding-center motion in the vacuum field of TMNS. Such calculations ignore the effect of finite β on field-line curvature in the transition section where the radial displacement takes place, but should give reasonable estimates of the magnitude of the displacement. The deflection δr for $r = 40$ cm is plotted vs. $\epsilon_\parallel / \epsilon$ at $\epsilon = 3.52$ MeV in Fig. 6 for a particular magnet design for TMNS (MAF/03B). We note a maximum $|\delta r/r|$ of about .140 occurring near the loss cone. The negative δr occurs because of the direction of

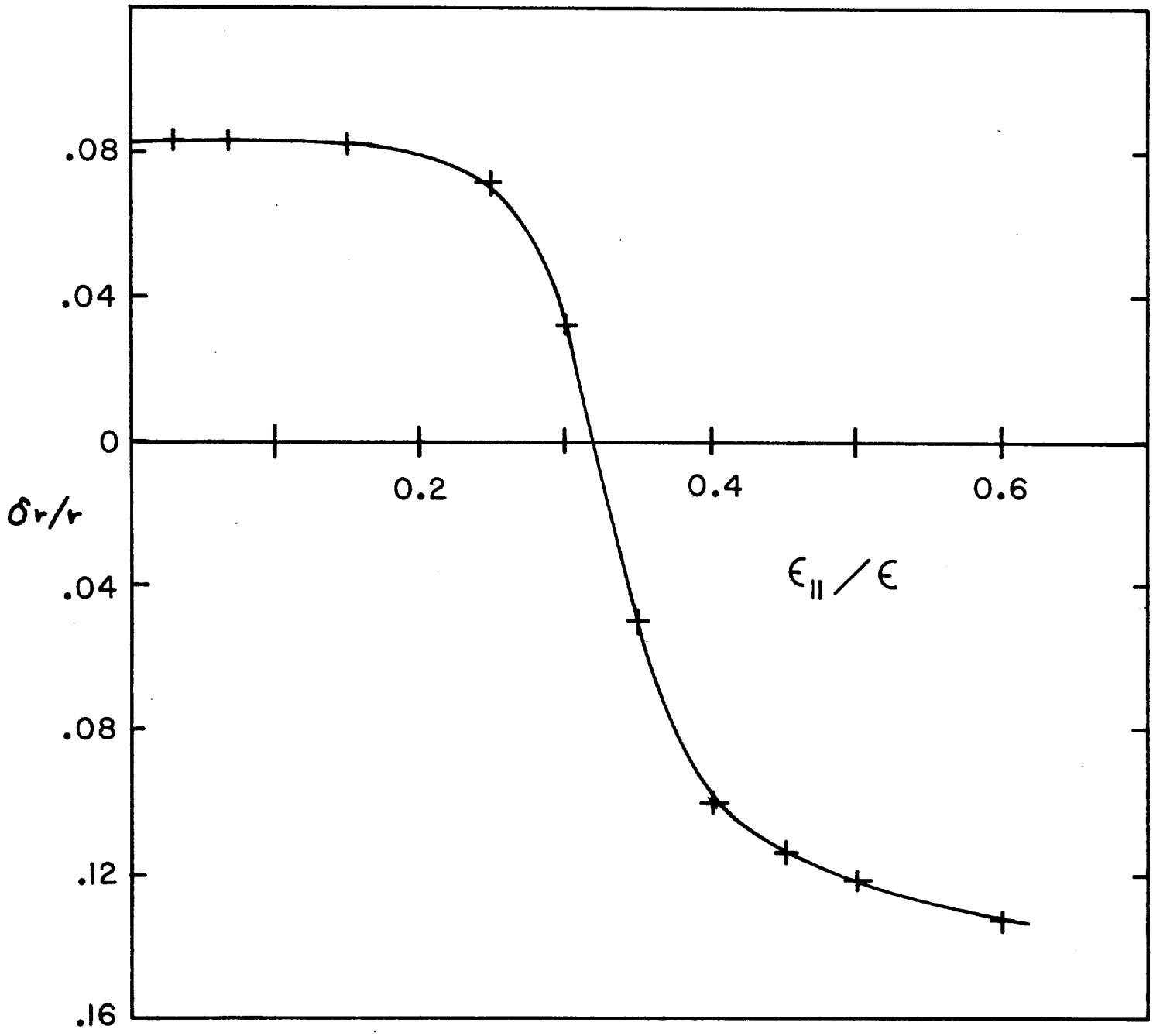

Fig. 6 Radial deflection per bounce for 3.5 MeV alpha particle in TMNS vacuum field vs. $\epsilon_{\parallel} / \epsilon$.

the curvature vector at the end of the machine; rather surprising is the change in sign of δr (and also of the direction of azimuthal drift) near $\epsilon_{\|}/\epsilon = .4$. This feature arises because the particular combination of axisymmetric and quadrupole fields for this design causes the curvature to change sign part way through the transition section. This particular magnetic field design also allows the quadrupole field to penetrate too far into the central cell, as reflected by the finite $\delta r/r$ for $\epsilon_{\|}/\epsilon \sim 0$. Calculations at other radii display the same behavior as Fig. 6; values for lower energy may be found from the scaling $\delta r/r \sim \sqrt{\epsilon}$

From the curve in Fig. 6 and Eq. (15), we compute values for ξ as listed in Table II. We see that stochastic diffusion should not be a problem for TMNS, providing a step in the axisymmetric field is introduced to eliminate the higher-k resonances. The criterion of Ineq. (14) is sensitive to L_c; raising L_c to 100 m, a typical value for a reactor could bring stochastic behavior for k = 3 and $\epsilon \approx 3.5$ MeV.

The scaling relation (13) also applies to the resonant plateau regime. More favorable scaling occurs in the resonant banana regime,

$$D \sim r^2(\delta r/r)^2 \epsilon^{-3/2} \tag{16}$$

The latter is valid under the approximate conditions

$$\nu_\alpha \tau_b < (\delta r/r)^{3/2} \tag{17}$$

where ν_α is the collision frequency for alpha-fuel ion interactions, given approximately by

$$\nu_\alpha = \frac{7.2 \times 10^{-12}\ n_i}{\epsilon^{3/2}} \tag{18}$$

for n_i in m^{-3} and ϵ in eV. Inequality (17) can be rewritten in the form

$$V_{\parallel} > \frac{7.2 \times 10^{-12}\ n_i\ L_c}{|\delta r/r|^{3/2}\ \epsilon^{3/2}} \tag{19}$$

This (approximate) boundary is indicated in Fig. 5. We see that only the thermalized alphas will be in the resonant plateau regime (fuel ions are also in this regime). Thus, even if only a very slight axisymmetric mirror is employed and several resonances remain, the alpha particles are expected to survive quite well to thermal energies. Total alpha particle energy deposition fraction of 60 - 80% appears possible.

IV. Magnetic Field in the Tandem Mirror Next Step (TMNS)

We make a simple magnetic field model based upon the long-thin approximation. This model saves computational time and enables us to easily obtain the gradient of magnetic field for calculating the drift orbits of alpha particles in the TMNS. In this approximation, the vacuum magnetic field is given by [6],

$$B_x = -\frac{x}{2}(f' - g), \tag{20a}$$

$$B_y = -\frac{y}{2}(f' + g), \tag{20b}$$

$$B_z = f, \tag{20c}$$

where f and g are arbitrary functions of z which specify the shape of the axisymmetric and quadrupole fields. Once we obtain equations for f and g, the magnetic field can be produced by the above equations. The constant flux surfaces are also given by

$$x^2 e^{-\eta(z)} + y^2 e^{\eta(z)} = r^2 \tag{21}$$

where $\eta(z)$ is defined by

$$\eta(z) \equiv \int_0^z \frac{g(t)}{f(t)}\, dt \tag{22}$$

$e^{\eta(z)}$ stands for the ellipticity of the cross section of the plasma. The derivative of Eq. (22) gives the following equation,

$$g(z) = \eta'(z)\, f(z). \tag{23}$$

Since f(z) corresponds to the magnetic field magnitude on the magnetic axis, we get the numerical values from the results of EFFI code[2] as shown in Fig. 7 with the first and second derivatives of f(z) calculated from the data by difference formulae.

In order to get the values of g(z), i.e., $\eta(z)$ through Eq. (22), we take a specific field line passing through the point $(r_0,0,0)$ in x-y-z coordinates,

$$x = r_0[f(0)e^{\eta(z)}/f(z)]^{1/2} \tag{24}$$

The numerical values of x-coordinates of the field line are given by EFFI code. Hence, the values of $\eta(z)$ can be obtained by,

$$\eta(z) = \ln\left[\frac{x^2}{r_0^2}\,\frac{f(z)}{f(0)}\right] \tag{25}$$

The numerical values of $\eta(z)$ are shown with the derivatives in Fig. 8. We can compute, based upon these numerical data, the coefficients of the cubic spline functions using the least square approximation by the cubic splines with variables knots and produce the functions, f, η and their derivatives. In producing the magnetic field by Eqs. (20a-c), we should note the following relations.

(i)	$z < -z_1$	$f(z) = f(\|z\|), \eta(z) = -\eta(\|z\|)$
(ii)	$-z_1 \leqq z \leqq -z_0$	$f(z) = B_s, \eta(z) = -\eta(\|z\|)$
(iii)	$\|z\| < z_0$	$f(z) = B_s, \eta(z) = 0$
(iv)	$z_0 \leqq z \leqq z_1$	$f(z) = B_s, \eta(z) = \eta(\|z\|)$
(v)	$z > z_1$	$f(z) = f(\|z\|), \eta(z) = \eta(\|z\|)$

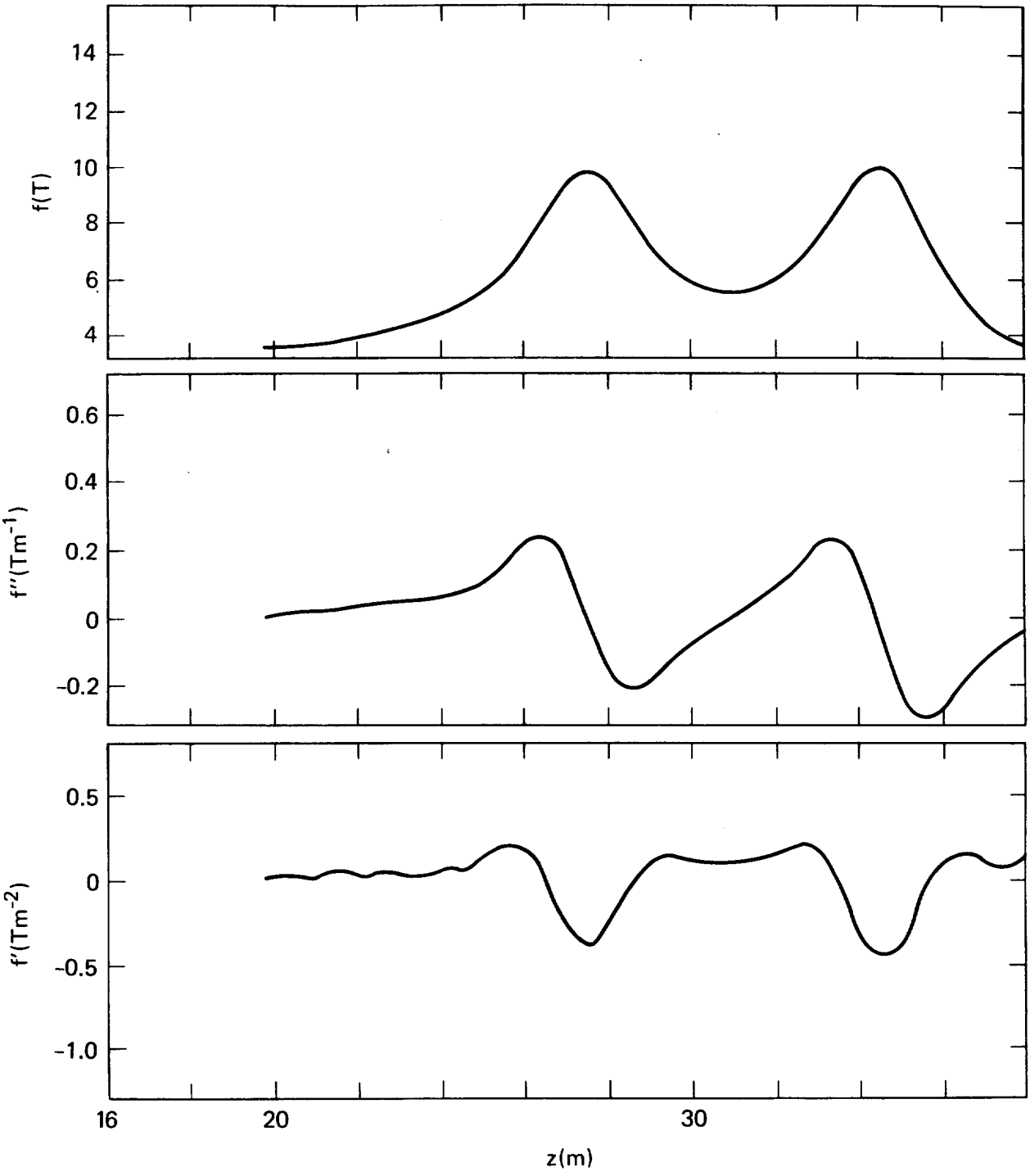

Fig. 7 Magnetic field magnitude on the magnetic axis, f(z) and the first and second derivatives, f'(z) and f"(z) in the TMNS.

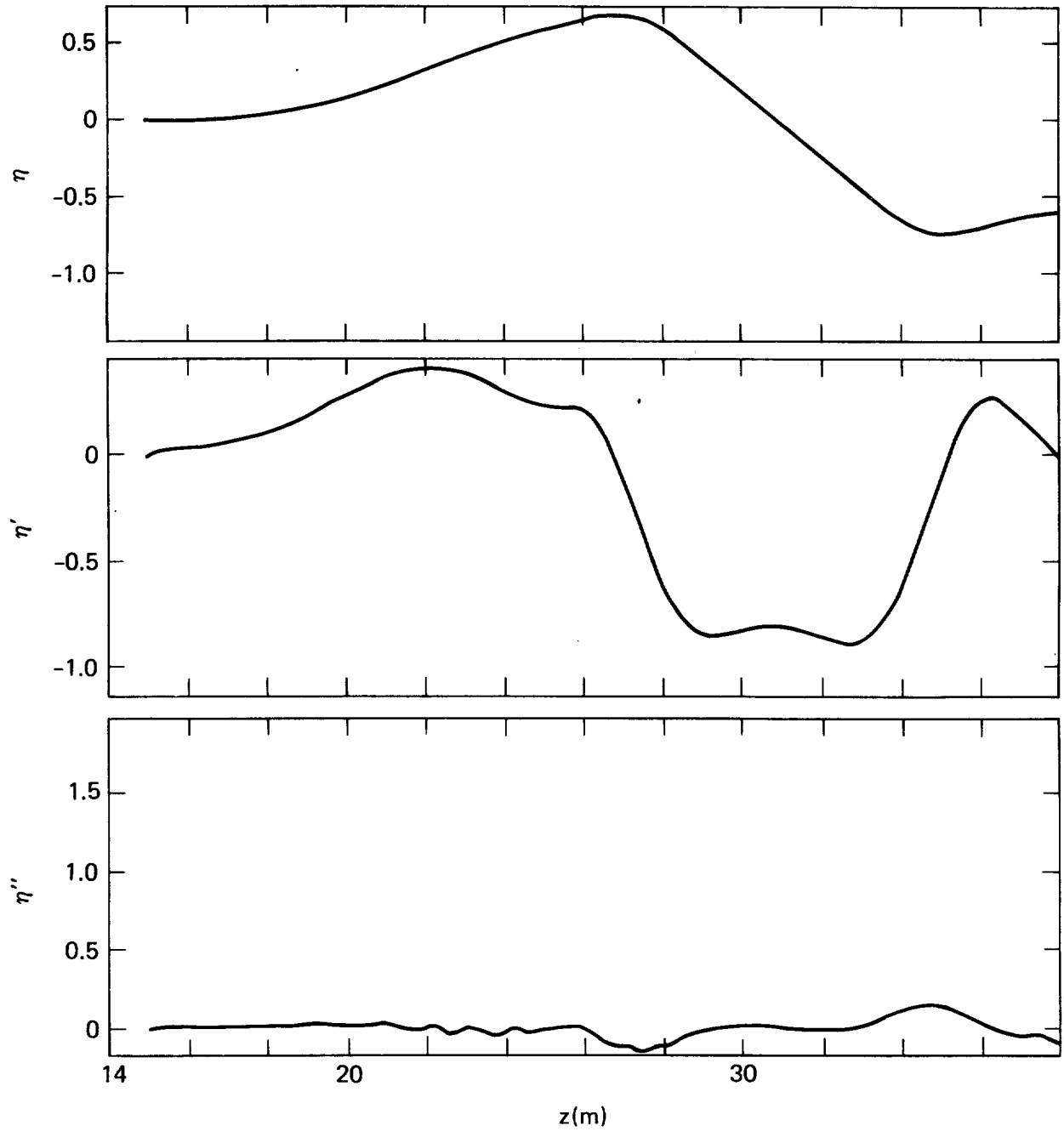

Fig. 8 Values of $\eta(z)$ related to the ellipticity and the derivatives, $\eta'(z)$ and $\eta''(z)$ calculated by the difference approximation.

where z_0 and z_1 are the maximum values of z coordinates which satisfy the relations of $\eta(z) = 0$ and $f(z) = B_s$, respectively. The inequality $z_0 < z_1$ holds in the present magnetic field for the TMNS. Thus, the quadrupole field extends into the central cell, contrary to the recommendation of Section II.

Using this model, we can calculate the magnetic field line, the components of $\nabla \times \underset{\sim}{B}$, ∇B, etc. For example, a field line and the gradient of magnetic field on the field line are depicted in Fig. 9 and 10, respectively.

V. Typical orbits in the TMNS

The guiding center equations of motions are given by

$$\frac{d\underset{\sim}{v}_{\parallel}}{dt} = -\mu \frac{\nabla B}{m} \cdot \frac{\underset{\sim}{B}}{B} \tag{26}$$

and

$$\underset{\sim}{v}_d = \frac{\underset{\sim}{E} \times \underset{\sim}{B}}{B^2} + \frac{1}{ezB^2}\left[\mu \underset{\sim}{B} \times \nabla B + \frac{mv_{\parallel}^2}{B^2}\, \underset{\sim}{B} \times (\underset{\sim}{B} \times \nabla)B\right] \tag{27}$$

where $\underset{\sim}{v}_{\parallel}$ and $\underset{\sim}{v}_d$ are the velocities of an alpha particle guiding center parallel and perpendicular to the magnetic field. μ is the magnetic moment. Although the axial electric potential is assumed to be negligibly small compared with the alpha particle energy, the effects of radial electric field on the drift motion are taken into consideration. The plasma β is assumed to be so low that the gradient B drift caused by the finite beta effects can be safely neglected. The trajectories of alpha particles in the TMNS are obtained by solving Eqs. (26) and (27) under the TMNS magnetic field configuration and the appropriate initial conditions.[7]

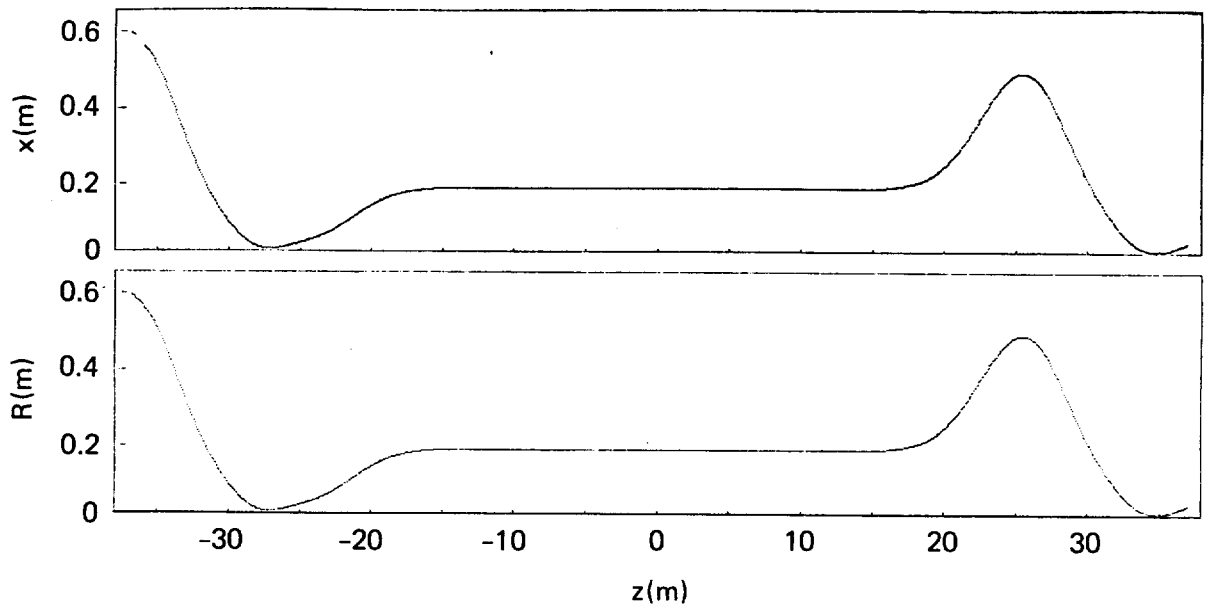

Fig. 9 Field line passing through the point (0.2,0,0). R stands for the distance from the magnetic axis.

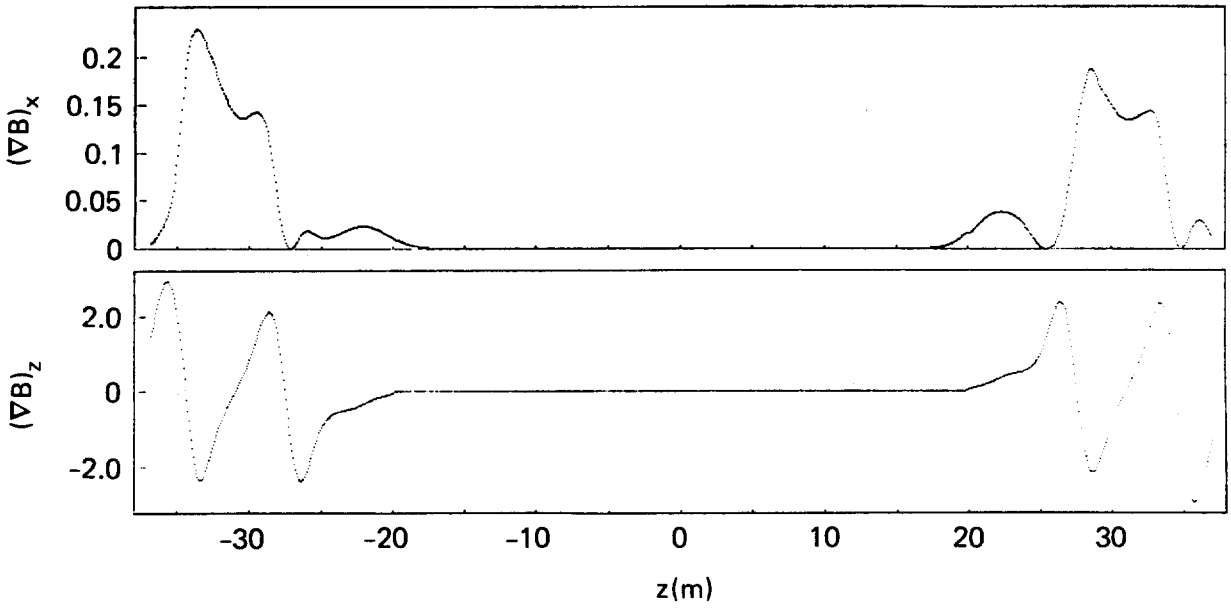

Fig. 10 Gradient of the magnetic field on the field line of Fig. 3.

Figure 11 shows the trajectories of a 3.5 MeV alpha particle projected onto the x-z, y-z, x-y and r-z planes. The pitch angle of the particle is very close to the loss cone angle in the central-cell mirrors. The particle is so barely trapped as to move deeply into the transition region and suffer from large radial deflection due to the quadrupole field. Since the velocity parallel to the magnetic field is much larger than the azimuthal velocity due to $\underset{\sim}{E} \times \underset{\sim}{B}$ drift, the angular deflection per bounce, $\delta \psi$, is very small. The particle deflected in at one end is deflected out at the other end due to the 90° mutual orientation of the quadrupole field. Figure 12 shows the trajectory projected along the field lines on to the mid-plane of the central cell. Although the drift surface of the particle deviates from the magnetic flux surface, the deviation is less than the Larmor radius. Then, this type of trajectory is not very important for the transport of alpha particles.

Figure 13 shows the trajectories of a deeply trapped particle, which rotates nearly 90° due to $\underset{\sim}{E} \times \underset{\sim}{B}$ drift per bounce and satisfies the $k = 1$ resonance condition. Incidentally, the pitch angle and energy of the particle are 85° and 3.5 MeV. The trajectory projected along the field lines onto the mid-plane are shown in Fig. 14. We can recognize the considerable deviation of the drift orbit from the magnetic surface. Figure 15 shows the positions (denoted by dots) and the directions (denoted by plus and minus) of the particle in crossing the mid-plane of the central cell. Although the results look random, we get the banana orbit, shown in Fig. 16, by rotating the successive points in Fig. 15 onto the first quadrant. The orbit is the so-called resonance banana and

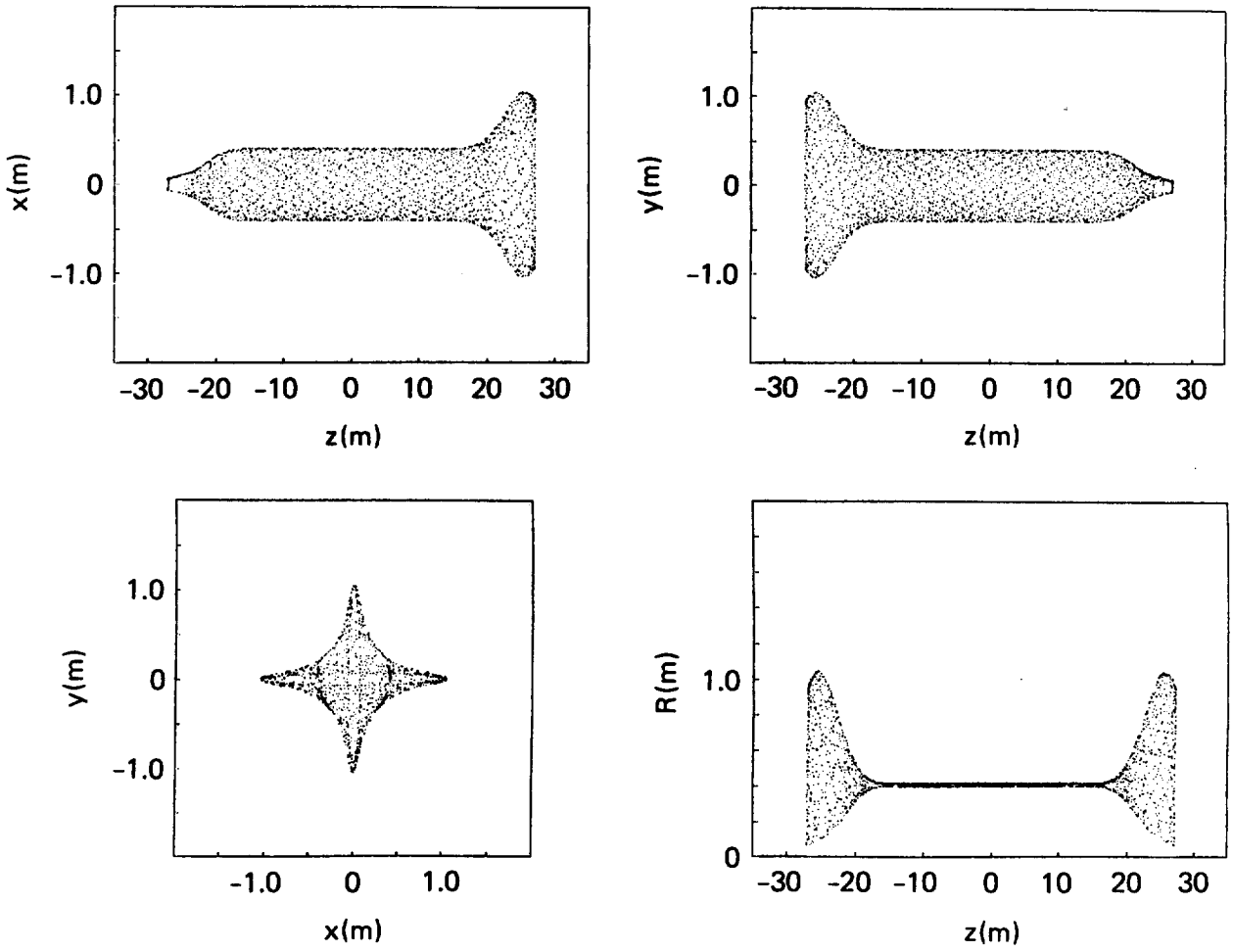

Fig. 11 Projections of 3.5 MeV alpha particle trajectory onto the x-z, y-z, x-y and r-z planes.

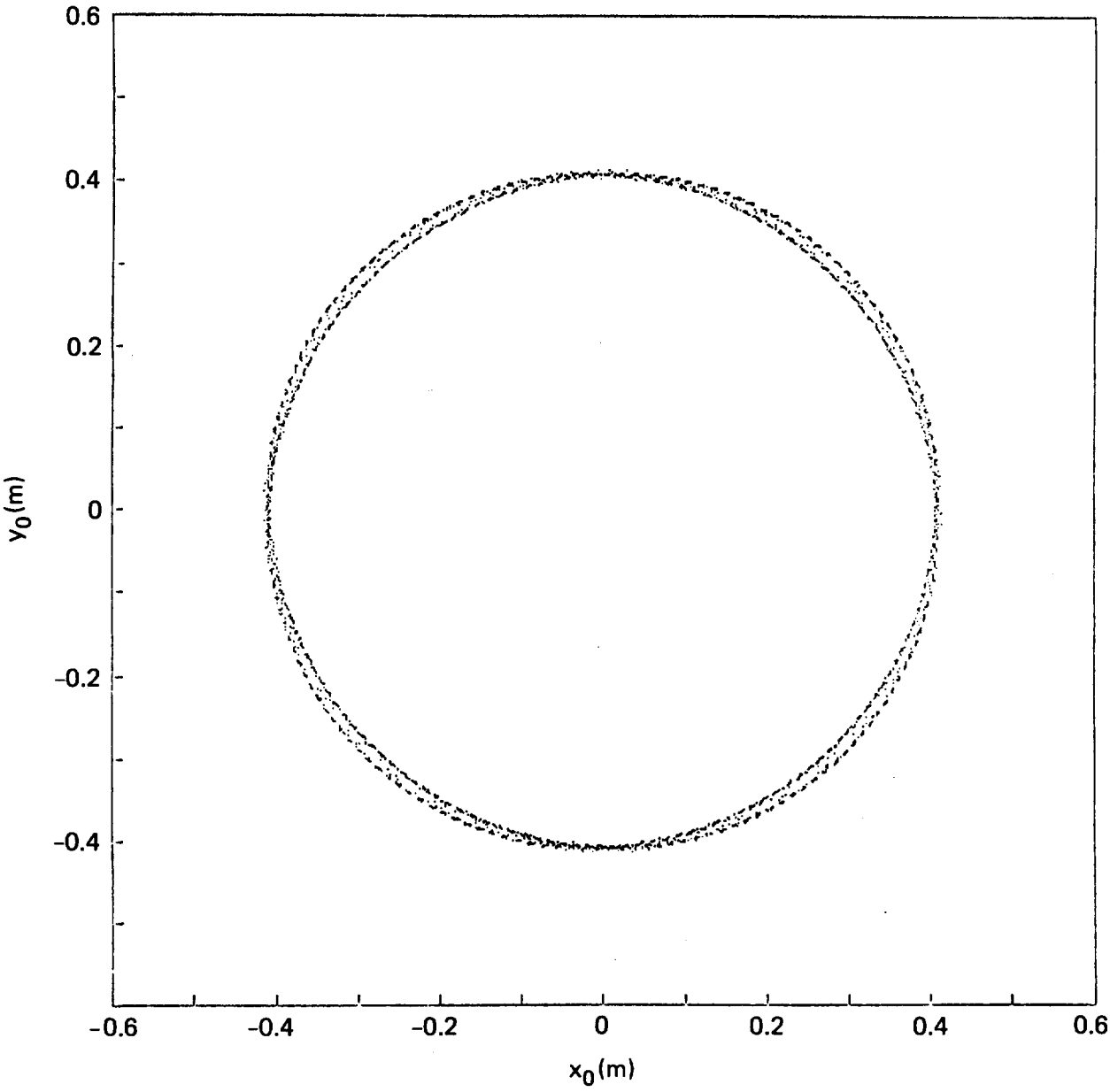

Fig. 12 Projection along the field lines onto the mid-plane of the central cell.

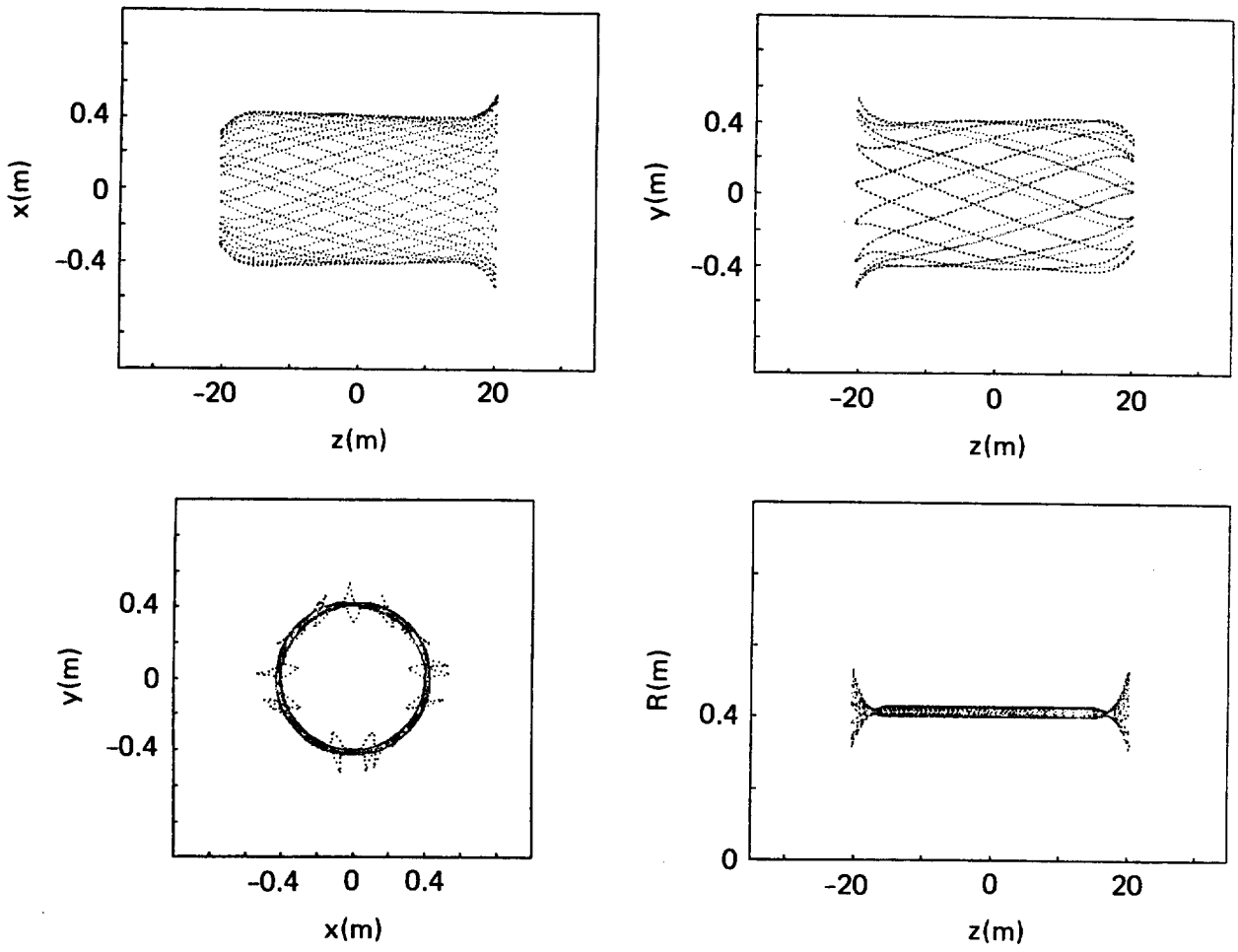

Fig. 13 Projections of trajectory of a deeply trapped particle, which presents the resonance (k = 1) behavior.

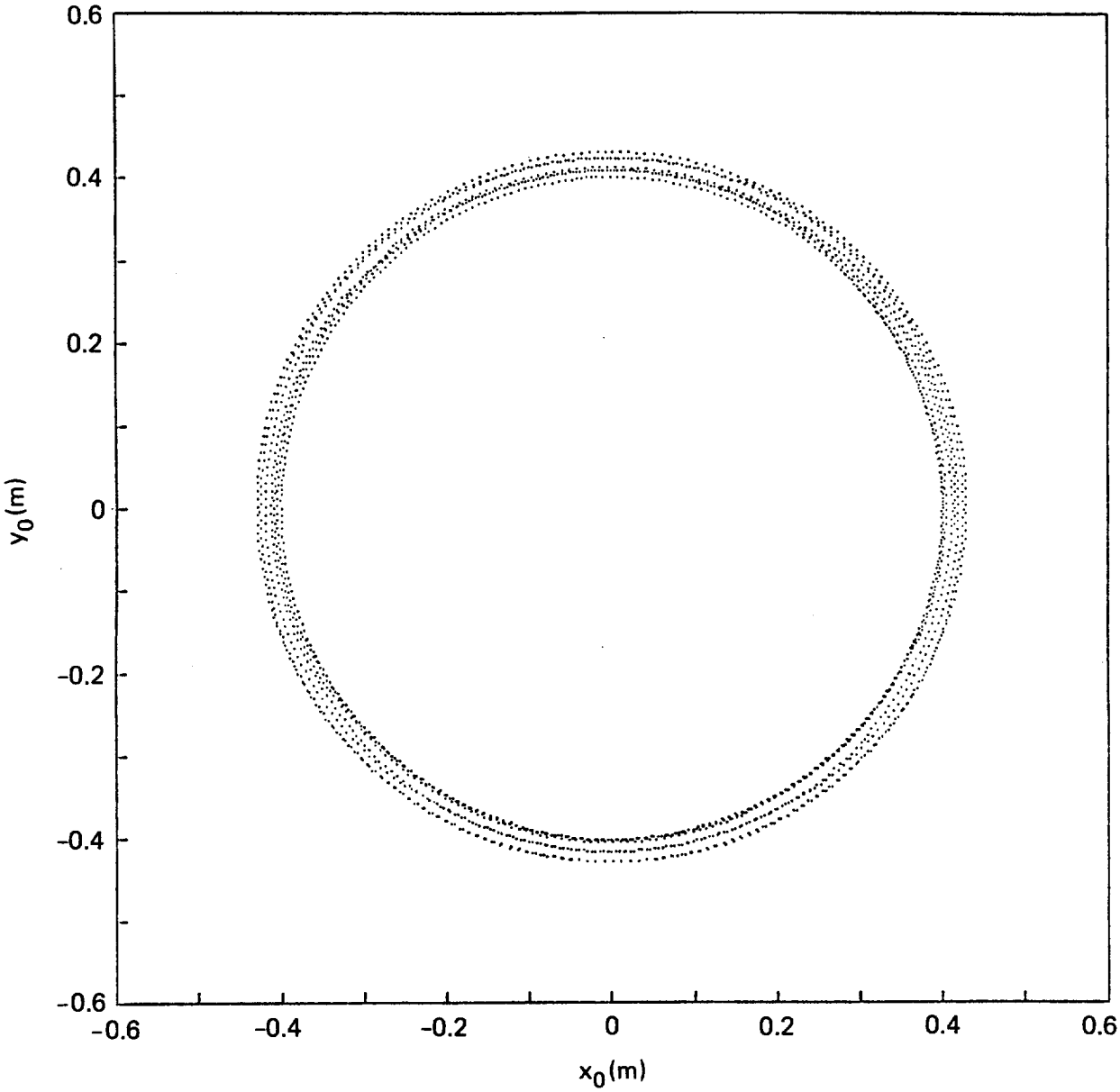

Fig. 14 Projection of the resonance orbit along field lines into the mid-plane of central cell.

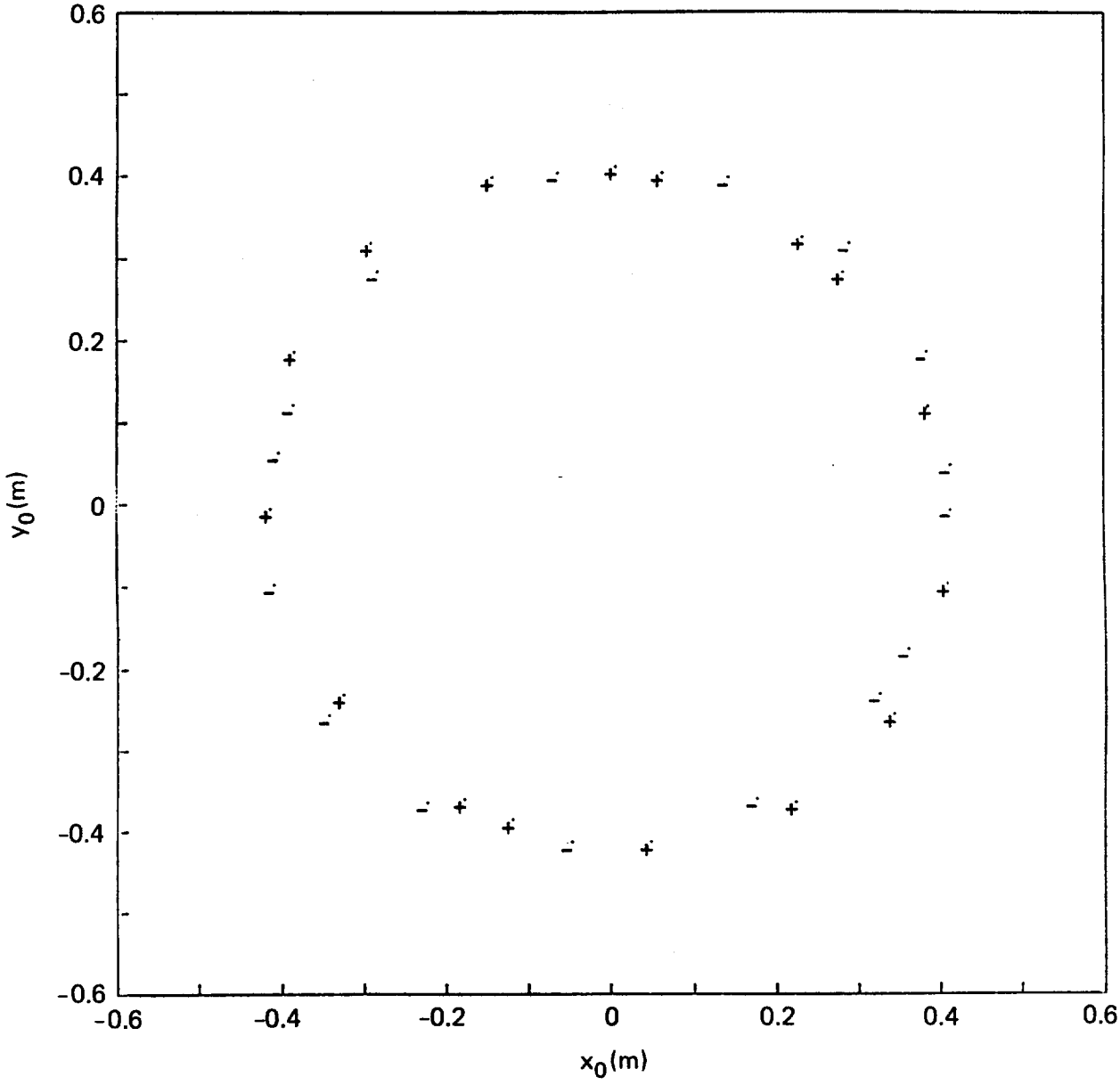

Fig. 15 Positions and directions of the guiding center in crossing the mid-plane of the central cell.

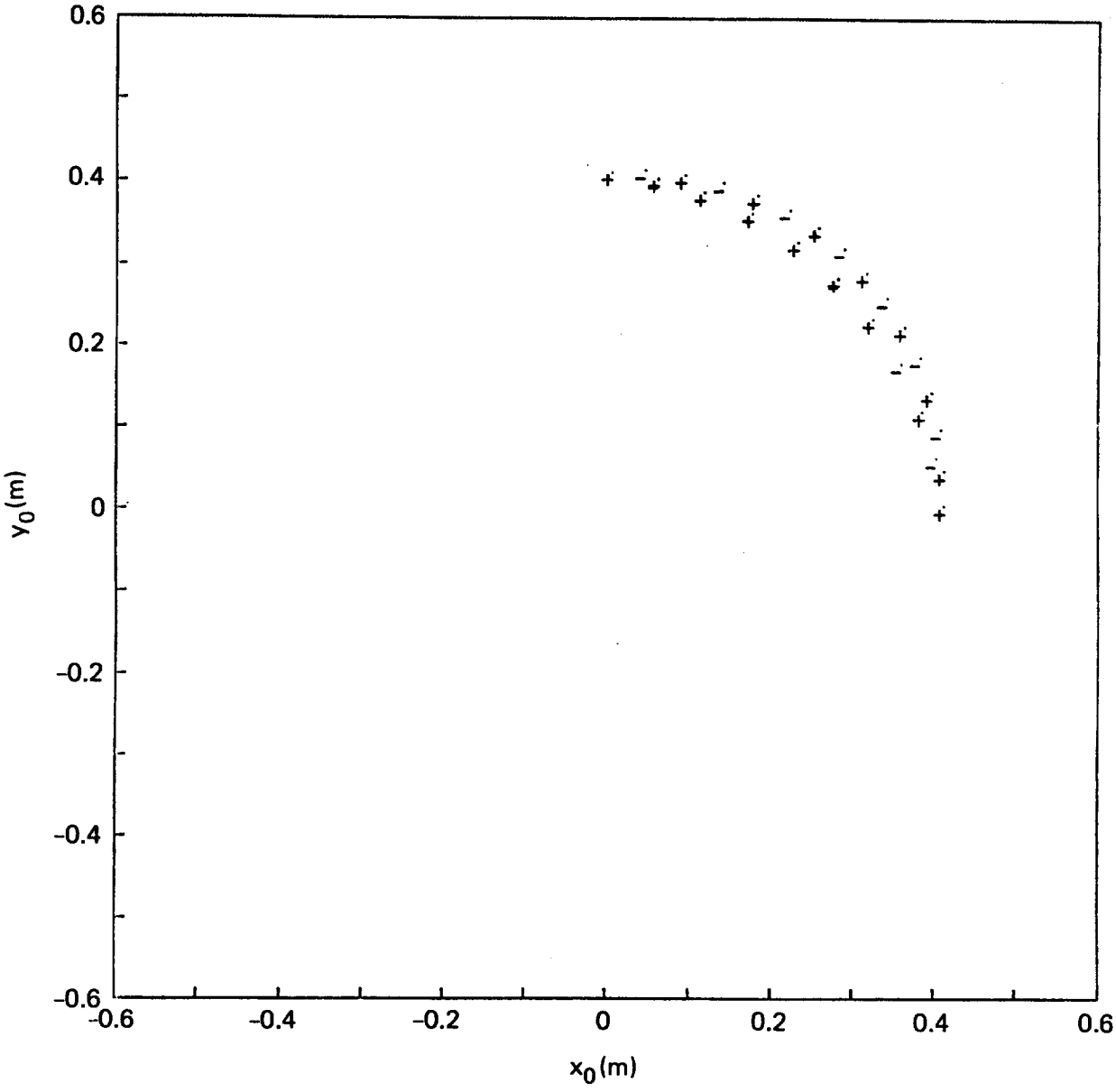

Fig. 16 Resonance banana orbits, obtained by mapping the crossing points shown in Fig. 15 onto the first quadrant.

its width is comparable to or larger than the Larmor radius. As discussed previously, this type of trajectory plays an important role in the transport of alpha particles. Further development of the computer code to include finite β effects on drift is underway.

REFERENCES

1. D. D. Ryutov and G. V. Stupakov, JETP Letters 28, 174 (1977); Sov. Phys. Dokl. 23, 412 (1978)

2. S. J. Sackett, LLL UCRL-52402 (1978)

3. M. E. Rensink, R. W. Cohen and A. A. Mirin, in LLL UCID-18496-Part 2 (1980)

4. D. E. Baldwin, LLL UCID-17926 (1978)

5. R. S. Devoto (unpublished)

6. J. C. Riordan, A. J. Lichtenberg, M. A. Lieberman, Nuclear Fusion, 19, (1979) 21.

7. The coding of Eqs. (26)-(27) was carried out by John Kerns (Rensselaer Polytechnic Institute).

Table I. Representative Parameters for TMNS

β_o	= 0.5	B_v	= 3.5T
L_c	= 30 m	r_p	= 54 cm
T_e	= 40 keV	n_o	= $1.4 \times 10^{14} cm^{-3}$
B_m	= 9.5T	R	= 3.64

Table II. Values of $\xi \equiv |\delta r||\partial \Delta\psi/\partial r|$ for various resonances at 3.5 MeV

k	10 cm	20 cm	40 cm	60 cm
1	.2	.2	.1	.04
3	.8	.7	.3	.2
5	2	1.2	.6	.3
7	-	1.6	.8	.4